British Journal of Applied Science & Technology
15(3): 1-8, 2016, Article no.BJAST.22787
ISSN: 2231-0843, NLM ID: 101664541

SCIENCEDOMAIN *international*
www.sciencedomain.org

An Algorithm of Finding Effective Distribution of Sub-elements in Overlay Model

S. M. Humayun Kabir[1*] and Tae-In Yeo[2]

[1]Department of Mechanical Engineering, Chittagong University of Engineering and Technology, Chittagong-4349, Bangladesh.
[2]School of Mechanical and Automotive Engineering, University of Ulsan, P.O. Box 18 Ulsan 680-749, Republic of Korea.

Authors' contributions

This work is carried out in collaboration between both authors. Author SMHK participated in analysis and writing the manuscript. Both authors read and approved the final manuscript.

Article Information

DOI: 10.9734/BJAST/2016/22787
Editor(s):
(1) Grzegorz Golanski, Institute of Materials Engineering, Czestochowa University of Technology, Poland.
Reviewers:
(1) Hui Yang, Beijing University, China.
(2) Ruben Dario Ortiz Ortiz, University of Cartagena, Colombia.
Complete Peer review History: http://sciencedomain.org/review-history/13896

Original Research Article

Received 27th October 2015
Accepted 18th November 2015
Published 28th March 2016

ABSTRACT

The idea of overlaying sub-elements in the inelastic constitutive models is studied. The main objective of this study is to propose an algorithm to find the effective distribution of sub-elements in Overlay model. In the course of study, experimental cyclic inelastic responses of a ferritic stainless steel are also illustrated in a brief. Proposed algorithm of searching effective distribution of sub-elements is based on an energy method where the percent of error is calculated. Depending on the number of sub-elements and error band, optimal distribution is achieved by adjusting some variables. For validation, numerical simulation is to be done using calculated material parameters. Correlation between experimental and simulated hysteresis loop is to be found successful.

Keywords: Overlay model; master curve; distribution of sub-elements; material parameters.

**Corresponding author: E-mail: dalimuou@yahoo.com;*

1. INTRODUCTION

Accurate presentation of inelastic responses of engineering components depends on optimization of parameters of constitutive models and robust analysis method. Various theoretical constitutive models based on continuum mechanics have been developed for describing the material nonlinearities under cyclic loading conditions. The literature in the arena of time-independent plasticity is vast. A few representative inelastic constitutive models concerning distributed-element model is cited only. The idea of overlaying sub-elements is first introduced by Masing in 1923 [1] in order to simulate the hardening of metallic materials. In order to describe creep and Bauschinger effect, Besseling [2] introduce a rheological model where an element of volume is considered to be composed of various sub-elements. Iwan [3] proposes the distributed-element for hysteretic analysis of structure. Later, Schiffner [1] introduced the different types of sub-elements (namely E, P, K, and I sub-element) for structural analysis under cyclic loading. Owen et al. [4] used a multi-linear model for the description of the stress–strain relationship, known as overlay model, where the uniaxial stress-strain response is represented by several linear segments. Distribution of sub-elements concepts is described in detail in other published literature [5]. And later the Overlay model is modified to consider the characteristics of cyclic deformation behavior of non-Masing material and strain range dependency [6]. Different phenomena regarding cyclic inelastic responses describe well in a brief somewhere else [7]. Selection of distribution of sub-elements is chosen arbitrary in the literature [6]. As optimized parameters play a crucial role in achieving better simulation, systematic determination of model parameters with the understanding of their physical significance is emphasized in this research. Therefore, the emphasis is put on presenting an algorithm to find the effective distribution of sub-elements effectively in modified Overlay model. For validation of the algorithm, attempts are to be made to simulate the stabilized hysteresis loops of a structural steel for the considered elasto-plastic constitutive models using the determined material parameters. Hence, experimental results of a ferritic stainless steel are also presented in brief.

The paper is organized as follows: Section 2 briefly shows the experiment results. Section 3 concisely describes the adopted constitutive models. Thereafter, a presentation of algorithm to find the effective distribution of sub-elements is presented in section 4. Numerical simulation of inelastic responses of materials using the parameters associated with proposed distribution of sub-elements is shown also in this section. Finally, conclusions have been drawn in Section 5.

2. EXPERIMENT AND RESULTS

The material used in this study is of 400-series ferritic stainless steel having a chemical composition of (in wt.%): 0.015 C; 1.00 Si; 0.04 P; 0.03 S; 15.00 Cr; 1.00 Mn; 1.65 Mo; 0.50 Nb. A closed-loop servo-hydraulic test system with 10ton capacity is used to conduct monotonic tensile test and low-cycle fatigue test. Test specimen of as-received material is designed in accordance with ASTM E606-92 standard having a diameter of 6 mm for tensile test and 8 mm for low cycle fatigue test with gage length of 12 mm. The tensile tests are carried out at a constant cross-head 4.8 mm/min corresponding to apparent strain rate of 2×10^{-3} /s. Isothermal low-cycle fatigue tests are carried out under fully-reversed total strain control applying a triangular waveform with a constant strain rate of 2×10^{-3}/s. The low-cycle fatigue test are performed at different total strain amplitude ranging from $\Delta\varepsilon/2$ = 0.3% to $\Delta\varepsilon/2$ = 0.7%. The displacement, load and strain signals are measured at each cycle. A 10% drop in the maximum load is defined as fatigue life. For detail experimental procedure, we can refer to other literature [8].

The evolution of peak stress is plotted against the applied cycles in Fig. 1 at different total strain amplitudes for the temperature of 200℃. All the curves illustrate a comparable sharp initial hardening between cycles one and ten, and gradual hardening is taken place for the rest of life at all strain amplitude except 0.3%. After an initial hardening, at strain amplitude of 0.3%, the material shows a distinct noticeable secondary hardening till the onset of the final load drop. Different authors reported similar hardening in cyclic stress response of ferritic stainless steels [9,10], austenitic steel [11], duplex stainless steel [12], and pearlitic eutectoid steel [13]. Fig. 2 represents stabilized loops at different strain amplitude which are the representative examples of stable hysteretic response of the materials for the temperature considered. Fig. 2 reveals that stabilized stress amplitude increases with increase of strain amplitude. For the as-received material, evolution of stress amplitude with respect to accumulated plastic strain up to the stabilization at strain amplitude of 0.7% is shown in Fig. 3.

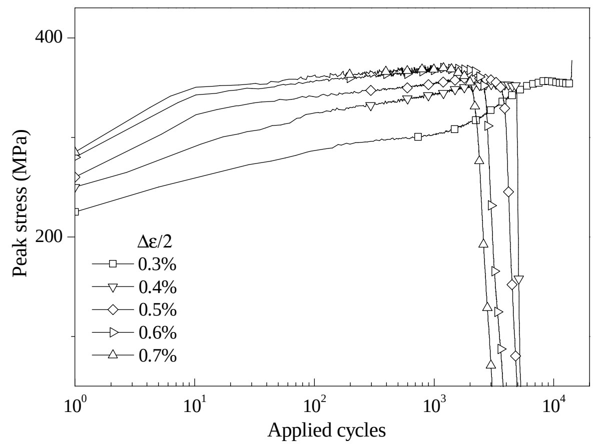

Fig. 1. Influence of strain amplitude on the evolution of peak stress

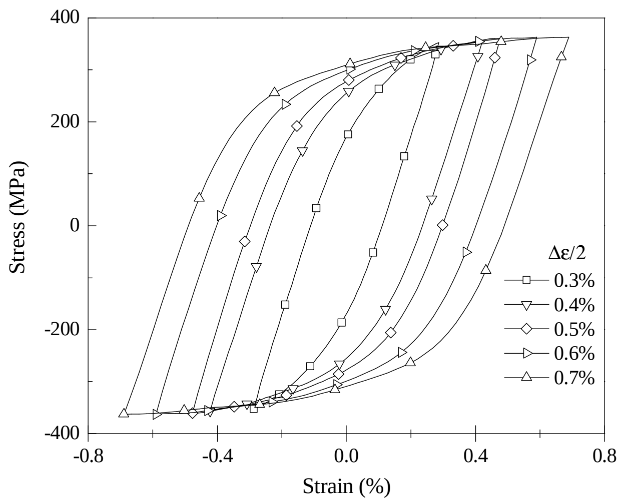

Fig. 2. Experimental hysteresis loops

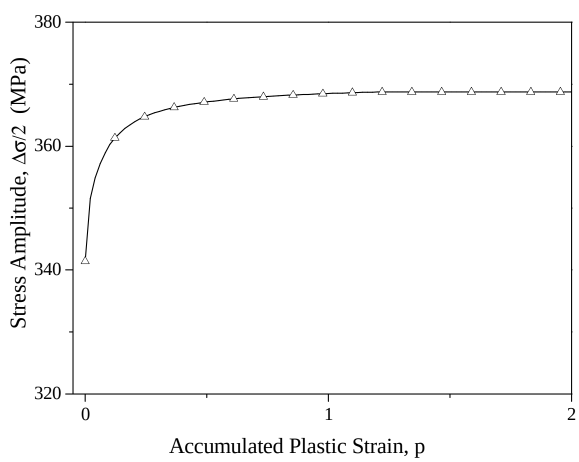

Fig. 3. Evolution of stress amplitude with respect to accumulated plastic strain

2.1 Overview of Overlay Model

The Overlay model is based on the assumption that the material is composed of a series of Jenkin's elements connected in parallel and each element consists of a linear spring with stiffness E_i in series with a slip element of strength k_i which is demonstrated in Fig. 4 [6]. Each element is therefore an ideal elasto-plastic unit as depicted in Fig. 5. The yield function of the sub-elements can be given as [3,6]

$$\tilde{f}_i = \sqrt{\frac{3}{2}}\left|\tilde{\boldsymbol{\sigma}}_i'\right| - k_i \quad (1)$$

Macroscopic stress is,

$$\boldsymbol{\sigma} = \sum_{i=1}^{N} \phi_i \tilde{\boldsymbol{\sigma}}_i \quad (2)$$

where, k_i, $\tilde{\boldsymbol{\sigma}}_i$, and ϕ_i defines the yield stress, applied stress tensor, and fraction of ith sub-element respectively. The stabilized hysteresis loops at different strain amplitudes are shifted to match the upper branch of every hysteresis loop so that the non-linear part of every hysteresis loop superimpose on a single common curve, called the master curve. A typical master curve is shown in Fig. 6. To evaluate the discrete distribution of elements, the tensile curve is divided into several linear segments to minimize the difference between a multi-linear curve and the original curve. The stiffness of the multi-linear curve is defined as,

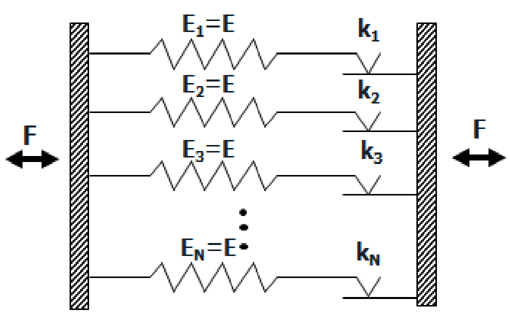

Fig. 4. The idea of overlaying sub-elements

$$\frac{\sigma_{i+1} - \sigma_i}{\varepsilon_{i+1} - \varepsilon_i} = \left(1 - \sum_{j=1}^{i} \phi_j\right) E \quad (3)$$

where, ϕ_i is yield fraction and $(\varepsilon_i, \sigma_i)$ is the ith vertex of the multi-linear curve.

2.2 Modified Overlay Model

To take into account the non-Masing's behavior of material and strain range dependency Overlay model was modified [6]. The yield stress is divided as follows,

$$k_i = m_i + R(\Delta\varepsilon, p) \quad (4)$$

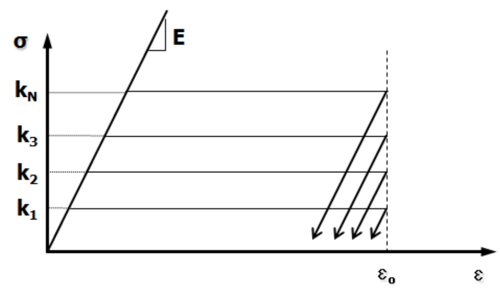

Fig. 5. The concept of elasto-perfectly plastic sub-elements for overlay model

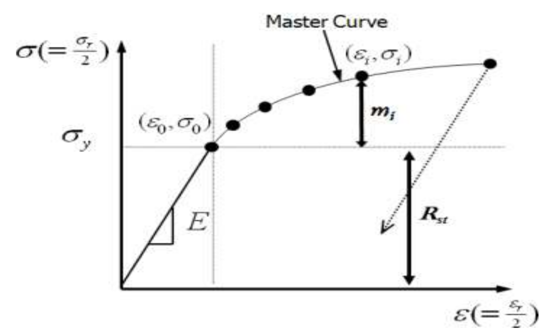

Fig. 6. Master curve

In Eq. (4), m_i represents parameters which describe the master curve shown in Fig.6 and $R(\Delta\varepsilon, p)$ represents the change of elastic limit which depends on the strain range $(\Delta\varepsilon)$ and accumulated plastic strain (p). For example, Fig. 7 shows the experimental stabilized hysteresis loops of Fig. 2 adjusted to lower peak. These loops are shifted so as to match the upper branch of every hysteresis loops for obtaining a master curve as in Fig. 8. When a few points $(\varepsilon_i, \sigma_i)$ are selected on master curve, the m_i and ϕ_i of each sub-element can be calculated through the Eqs. (5-6). In Fig. 8, σ_r is the reversed stress, ε_0 is the strain at the end of the elastic limit, ε_r is the reversed strain, and reversed elasto-plastic stress and strain are defined as $\sigma_{rep} = \sigma_r - 2R_{st}$ and $\varepsilon_{rep} = \varepsilon_r - 2\varepsilon_0$ respectively.

$$\phi_i = \frac{1}{E}\left(\frac{\sigma_i - \sigma_{i-1}}{\varepsilon_i - \varepsilon_{i-1}} - \frac{\sigma_{i+1} - \sigma_i}{\varepsilon_{i+1} - \varepsilon_i}\right) \tag{5}$$

$$m_i = E\varepsilon_i / 2 \tag{6}$$

Instead of choosing points on master curve i.e. selection of distribution of sub-elements arbitrary, we intend to develop an algorithm which is discussed in the next section. The evolution law of the elastic limit R in Eq. (4) in terms of the unified stress variation ratio can be represents as [14],

$$R = R_{st} + (R_{in} - R_{st})\exp(-bp) \tag{7}$$

where, R_{in} represents initial elastic limit R_0, R_{st} is elastic limit of the stabilized cycle, and b represent the stabilization curve steepness for the isotropic variables R.

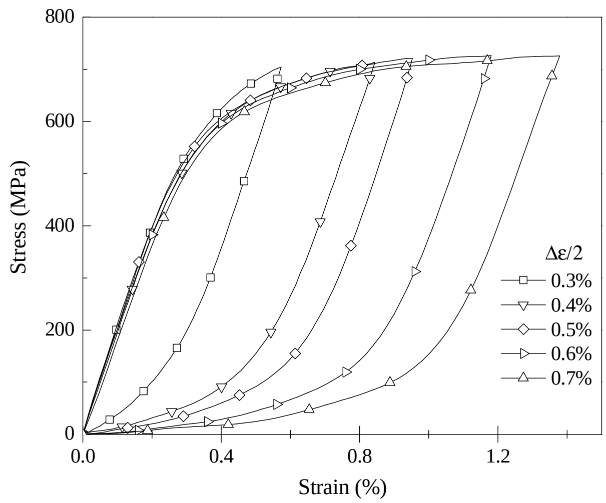

Fig. 7. Hysteresis loops adjusted to the lower peak

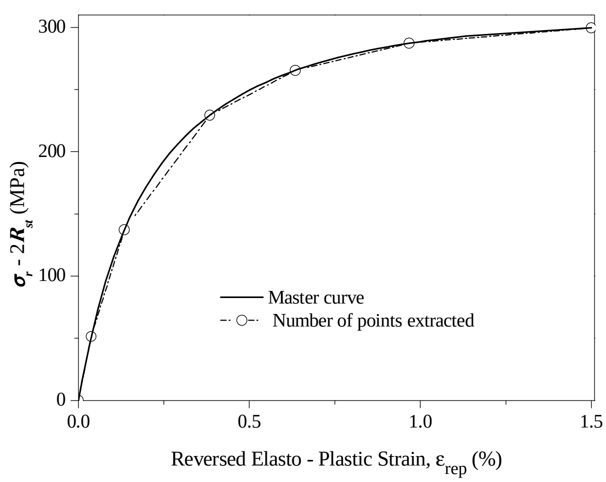

Fig. 8. Multi-linear segments of nonlinear master curve

3. OPTIMAL DISTRIBUTION OF SUB-ELEMENTS

To determine m_i 's and ϕ_i 's, we divide the nonlinear part of the upper branch of the stabilized hysteresis loop into six linear segments that minimize the difference between the original nonlinear curve and the multi-linear curve as in Fig. 8. Therefore, the number of sub-elements used here for the Modified Overlay model is six. In order to find out optimal distribution of sub-elements effectively i.e., find the location of points which divide the master curve into six linear segments, an algorithm (Fig. 9) based on energy method is employed where the percent of error is calculated by,

$$\theta = 1 - \frac{1}{2}(\sigma_{i+1} + \sigma_i)(\varepsilon_{i+1} - \varepsilon_i) / \int_{\varepsilon_i}^{\varepsilon_{i+1}} \sigma d\varepsilon \quad (8)$$

Depending upon the chosen numbers of points (n) on the master curve and the error (θ) between two successive points, initial increment of transposed plastic strain and both initial limits of error change to provide the optimum positions of the points on the master curve as shown in the algorithm (Fig. 9). As a result the distribution of sub-elements can be obtained effectively from the master curve. For this instance, the lower of

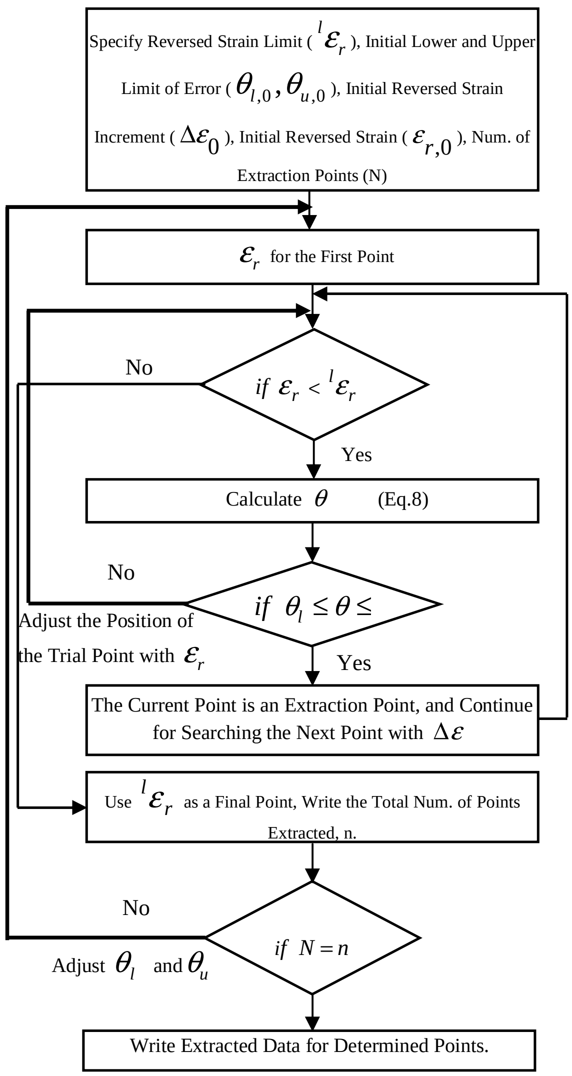

Fig. 9. Flow chart for extraction of required points with minimum error

error (θ_l) and upper limit of error (θ_u) in percent are 0.5 and 2.0. The kinematic parameters m_i's and ϕ_i's are computed from experimental stabilized loop data by means of Eq. (5) and Eq. (6) which are provided in Table 1. Isotropic hardening parameter b is determined by nonlinear regression procedure using Fig. 3. And other isotropic hardening parameters, R_0 and R_{st}, are determined systematically and efficiently for adopted steels in a similar fashion described in published literature [14]. Isotropic hardening parameters are listed in Table 2.

An attempt is made to simulate stabilized hysteresis loop using the parameters obtained. For numerical simulation, an axisymmetric version of the cylindrical sample is employed. Only one finite element in the middle of the sample is submitted to an imposed strain $\Delta\varepsilon/2 = \pm 0.007$ and subsequently analysis is carried out in ABAQUS with UMAT subroutine. Fig.10 illustrates that the prediction of stabilized loops coincides well with the experimental result. By adjusting a suitable numbers of overlays and by assigning optimum material properties, for example elasticity (E) and plasticity (R, m_i, ϕ_i, and so on), to different rheological units, we can simulate the hysteretic responses as closely as possible.

Table 1. Kinematic parameters regarding overlay model

N	m_i(MPa)	ϕ_i
0	0.00	0.2216
1	33.01	0.2744
2	118.21	0.2943
3	338.13	0.1280
4	558.05	0.0444
5	850.77	0.0241
6	1319.53	0.0132

Table 2. Determined isotropic parameters for elasto-plastic cyclic behavior

Temp. ℃	E (GPa)	R_0 (MPa)	b	R_{st} (MPa)
200	175.93	189.69	10.43	217.02

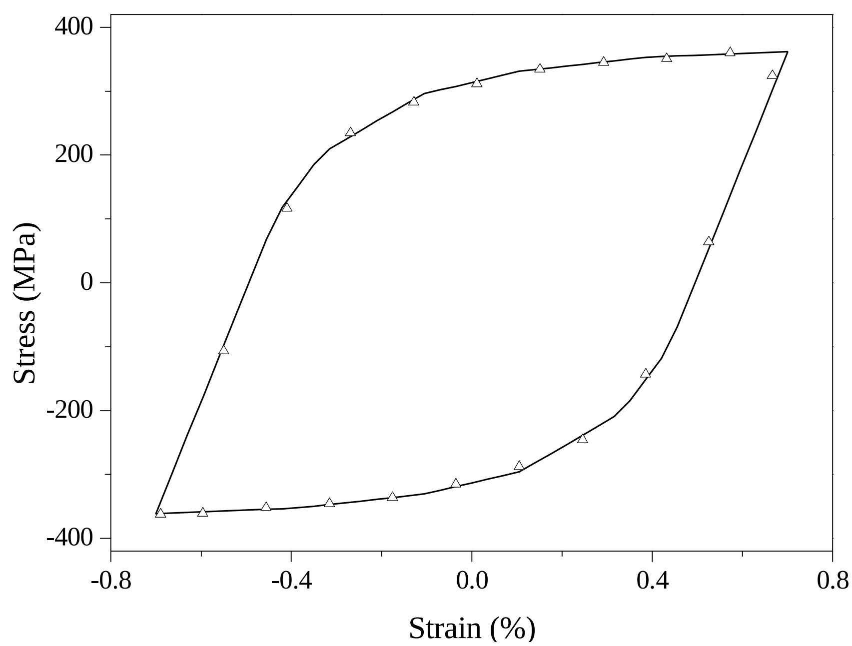

Fig. 10. Comparisons of stabilized hysteresis loops (solid lines: numerical simulation, symbols: Experimental data)

4. CONCLUSION

Overlay model has been studied for the ferritic stainless steel considered. Experimental results reveal that the material experiences hardening in general. For particular strain amplitude, a secondary hardening takes place till the onset of the final load drop after an initial hardening. An algorithm to find the effective distribution of sub-elements effectively in modified Overlay model is presented. In this approach, numbers of points on the master curve is chosen and lower and upper limit of errors are given. Searching optimal distribution of sub-elements is achieved by adjusting initial increment of transposed plastic strain and both initial limits of error. Material parameters are extracted and utilized in FE simulation. Numerical simulation is found in good agreement with experimental stabilized hysteresis loop.

COMPETING INTERESTS

Authors have declared that no competing interests exist.

REFERENCES

1. Schiffner K. Overlay models for structural analysis under cyclic loading. Comput Struct. 1995;56:321-328.
2. Besseling JF. A theory of elastic, plastic and creep deformations of an initially isotropic material showing anisotropic strain-hardening, creep recovery, and secondary creep. J Appl Mech. Trans ASME. 1958;25:529-536.
3. Iwan WD. A distributed-element model for hysteresis and its steady-state dynamic response. J Appl Mech. Trans ASME. 1966;893-900.
4. Owen RJ, Prakash A, Zienkiewicz OC. Finite element analysis of non-linear composite materials by use of overlay systems. Comput Struct. 1974;4:1251-1267.
5. Chandrakant S. Desai. Mechanics of materials and interfaces. CRC Press; 2001.
6. Yoon S, Hong SG, Lee SB. Phenomenological description of cyclic deformation using the overlay model. Mat Sci Eng. A. 2004;364:17-26.
7. Halama R, Sedlák J, Šofer M. Phenomenological modeling of cyclic plasticity. In Miidla P, Editor. Numerical Modelling. Intech; 2012.
8. Kabir SMH, Yeo T. Influence of temperature on a low-cycle fatigue behavior of a ferritic stainless steel. J Mech Sci Technol. 2014;28(7):2595-2607.
9. Avalos M, Alvarez-Armas II, Armas AF. Dynamic strain aging effects on low-cycle fatigue of AISI 430F. Mater Sci Eng A. 2009;513-514:1-7.
10. Lee KO, Yoon S, Lee, SB, Kim BS. Low cycle fatigue behavior of 429EM ferritic steel at elevated temperatures. Key Eng Mater. 2004;261-263:1135-1140.
11. Srinivasan VS, Sandhya R, Valsan M, Rao KBS, Mannan SL, Sastry DH. The influence of dynamic strain ageing on stress response and strain-life relationship in low cycle fatigue of 316L(N) stainless steel. Scripta Mater. 1997;37(10):1593-1598.
12. Herenu S, Alvarez-Armas I, Armas AF. The influence of dynamic strain aging on low-cycle fatigue of duplex stainless steel. Scripta Mater. 2001;45:739-745.
13. Tsuzaki K, Matsuzaki Y, Maki T, Tamura I. Fatigue deformation accompanying dynamic strain aging in a pearlitic eutectoid steel. Mater Sci Eng A. 1991;142(1):63-70.
14. Kabir SMH, Yeo T. Characterization of unified material parameters in elasto-plastic continuum approach. I RE ME. 2010;4(5):507-517.

Peer-review history:
The peer review history for this paper can be accessed here:
http://sciencedomain.org/review-history/13896